A five-coordinate [2Fe-2S] cluster.

Fuchs, Michael G G; Dechert, Sebastian; Demeshko, Serhiy; Ryde, Ulf; Meyer, Franc

Published in:
Inorganic Chemistry

DOI:
10.1021/ic902559n

2010

Document Version:
Peer reviewed version (aka post-print)

A Five-Coordinate [2Fe–2S] Cluster

Michael G. G. Fuchs, Sebastian Dechert, Serhiy Demeshko, Ulf Ryde, Franc Meyer*

Institut für Anorganische Chemie, Georg-August-Universität, Tammannstrasse 4, 37077 Göttingen, Germany.
Department of Theoretical Chemistry, Lund University, Chemical Centre, P. O. Box 124, 221 00 Lund, Sweden.

RECEIVED DATE (will be automatically inserted after manuscript is accepted)

ABSTRACT A unique [2Fe–2S] cluster (**1**) with genuinely five-coordinate ferric ions has been synthesized and investigated both structurally and spectroscopically. The crystal structure of **1** as well as ^{1}H NMR data reveal that 2,6-bis(imidazol-2-yl)pyridine binds to the [2Fe–2S] core as a tridentate capping ligand. DFT calculations showing spin density on all coordinating atoms support this finding. **1** has also been characterized by Mössbauer and UV/vis spectroscopy, mass spectrometry, cyclic voltammetry and magnetic susceptibility measurements. Significant spectroscopic properties that make **1** distinct from conventional [2Fe–2S] clusters include a rather small quadrupole splitting of 0.43 mm/s and a remarkably positive reduction potential of −0.52 V vs. NHE.

Introduction

The coordination geometry of the metal ions in the vast majority of biological Fe/S clusters is distorted tetrahedral.[1-3] This situation is also found in various biomimetic complexes, where many of the structural ans electronic properties of the natural systems have been reproduced.[2] Yet the protein environment has more means to influence cluster properties than most of the small ligands hitherto used in synthetic coordination compounds, and some essential properties of naturally occurring Fe/S clusters (such as the redox potentials of [2Fe–2S] ferredoxins) have not been fully emulated yet.

Although reduction potentials and other properties of biomimetic [2Fe–2S] clusters can be tuned to a certain extent by variation of the ligand substitution,[4] these influences are not sufficient to accomplish the versatility exhibited by natural clusters. Probably the most prominent example is the exceptionally positive redox potential displayed by the Rieske type [2Fe–2S] clusters coordinated by two cysteines and two histidines; even though a structural analogue has recently been reported, the most important feature – the redox potential – is not comparable to that of the natural archetype.[5] Apart from the Rieske type clusters bearing histidine ligands it is mainly the [2Fe–2S] cluster in biotin synthase that has a distinct ligand sphere. One of the ligands is an arginine residue,[6] which is very unusual for biological metal ligation.[7] The low resolution of the crystal structure does not allow for definite assignment of the protonation state and the coordination mode of this arginine residue, but unusual interactions are conceivable, including bidentate arginine coordination and the involvement in various hydrogen bonds.

Coordination numbers greater than four have been observed at individual iron atoms in some [4Fe-4S] proteins,[6,8-12] and this was successfully mimicked in some site-differentiated synthetic [4Fe–4S] clusters.[13,14] However, interactions other than via the four terminal ligands have been explored only scarcely in synthetic [2Fe–2S] clusters, namely hydrogen bonding[15] and weak coordination by an additional donor atom.[16] The latter concept of secondary bonding interactions, inspired particularly by the potential bidentate coordination of arginine in biotin synthase,[17] is here extended towards [2Fe–2S] clusters containing iron atoms with genuine coordination number five.

A suitable tridentate capping ligand for the [2Fe–2S] core should be diprotic (since synthetic [2Fe–2S] clusters in their diferric state are usually stabilized by two anionic terminal ligands) and should provide a pre-organized pocket with three donor atoms that can bind equally. 2,6-bis(imidazol-2-yl)pyridine[18] (H_2L) was thus chosen as a promising ligand. As H_2L has been shown to give iron complexes whose reduction potential can be tuned by protonation of the non-coordinating N atoms,[19] the potential for investigating proton-coupled electron transfer reactions as observed in Rieske proteins was an additional incentive for the choice of this particular ligand scaffold.

Results and Discussion

When H_2L was treated with ^{n}BuLi or KH in DMF and $(NEt_4)_2[Fe_2S_2Cl_4]$[20] was subsequently added, the deep red color typical for [2Fe–2S] clusters was retained. Slow diffusion of Et_2O into a complex solution caused precipitation of a powder that showed the expected signals

in the ^{1}H NMR spectrum. In addition, crystals suitable for X-ray diffraction were obtained and the product could be identified as the target complex **1**. Due to gradual decomposition in DMF (and more so in DMSO) no pure bulk material could be obtained by recrystallization from DMF/Et_2O. However, when the synthesis was performed in THF/MeCN, **1** precipitated within a few hours and could be collected by filtration (Scheme 1); this material proved to be pure by NMR and Mössbauer spectroscopy. The main challenge in the synthesis is to avoid cluster degradation and formation of the undesired $[L_2Fe^{II}]^{2-}$ or $[L_2Fe^{III}]^{-}$ species (usually observed as major products with many related ligands), which requires optimization and meticulous control of the reaction conditions. **1** is only sparingly soluble but stable in MeCN, while it decomposes in DMF and DMSO solutions.

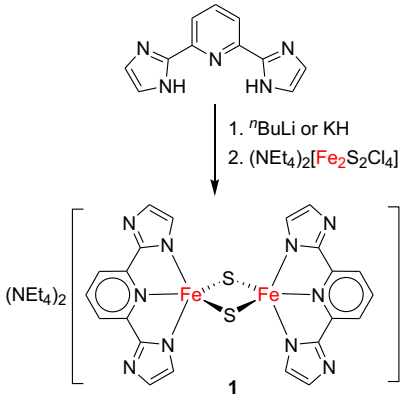

Scheme 1. Synthesis of Complex **1**.

The crystal structure of **1** shows an intact sulfide-bridged diferric cluster core coordinated by two ligands with a crystallographic C_2 symmetry axis through the [2Fe–2S] plane (Figure 1). Although the distances between the iron atoms and the imidazole N atoms are shorter (2.11 and 2.12 Å), the pyridine N atoms are clearly within bonding distance (2.18 Å). Compared to most other [2Fe–2S] clusters, the Fe· · · Fe distance in **1** is somewhat elongated to 2.79 Å, but is in the range previously observed for clusters with secondary bonding interaction (*cf.* 2.80 Å in a cluster with additional weak thioether coordination[16]). This goes along with an increase of the Fe–S–Fe angle to 77.7° compared to 74–76° for normal [2Fe–2S] clusters with four-coordinate metal ions.[2] The angle N1–Fe1–N4 in **1** (141.3°) deviates significantly from 180°, and the coordination geometry of the ferric ions is best described as square pyramidal with one of the bridging sulfide ions occupying the apical position. Accordingly the τ_5 value, which quantifies the degree of trigonality,[21] is close to zero (0.085). The Fe1–S1 bond involving the apical S atom (2.24 Å) is slightly longer than Fe1–S1' in the basal plane (2.21 Å). All relevant distances and angles are collected in Table 1.

Figure 1. Molecular Structure of **1**. ORTEP plot, with 50 % probability thermal ellipsoids; counterions and hydrogen atoms are omitted for clarity; only crystallographically independent heteroatoms are labelled.

The ^{1}H NMR spectrum of **1** in DMF-d_7 shows typically broad signals at 12.83 and 13.71 ppm for the imidazole protons and at 6.90 and 9.00 ppm for the pyridine protons (Figure 2). The pronounced broadening of the latter signal is further proof for genuine coordination by the pyridine moiety. The two imidazole signals appear at a remarkably low field compared to ligand signals in other N-coordinate [2Fe-2S] clusters.[22]

Figure 2. ^{1}H NMR spectrum of **1** recorded at 500 MHz in DMF-d_7.

The UV/vis spectrum of **1** resembles that of more conventional [2Fe–2S] clusters (Figure 3). Besides an intense band at 310 nm with a shoulder at 370 nm there is a band with much lower intensity in the visible region at 489 nm, presumably a charge-transfer absorption. Compared to clusters with tetrahedral metal ions bearing bidentate N-donor capping ligands,[22] both bands are shifted to higher energies.

Figure 3. UV/vis spectrum of cluster **1** in DMSO.

Cyclic voltammetry was performed in DMF solution (Figure 4). A quasi-reversible reduction at a surprisingly positive potential (midwave potential at –0.75 V vs. the $Cp^*_2Fe/Cp^*_2Fe^+$ couple or –0.52 V vs. NHE) and a further irreversible reduction (E^c_p at –1.37 V vs. the $Cp^*_2Fe/Cp^*_2Fe^+$ couple or –1.14 V vs. NHE[23]) was observed. Although clusters stabilized by NH· · · S hydrogen bonds exhibit even more positive reduction potentials, up to –0.35 V vs. NHE,[15] the potential of **1** is among the most positive found for synthetic [2Fe–2S] clusters and is almost in the range of [2Fe–2S] ferredoxins (–0.15 to –0.45 V).[3]

Figure 4. Cyclic voltammogram of **1** in DMF/$N^nBu_4PF_6$ (0.1 M) at 100 mV/s; calibrated vs. the $Cp^*_2Fe/Cp^*_2Fe^+$ couple as internal standard and referenced vs. NHE.[23]

The Mössbauer spectrum of **1** (Figure 5) shows a single quadrupole doublet with isomer shift δ = 0.44 mm/s which is rather positive compared to other N-coordinate [2Fe–2S] clusters; e.g., a cluster with methylindolate capping ligand shows δ = 0.29 mm/s.[24] While a linear correlation between the oxidation state *s* of the iron atoms and the isomer shift according to $\delta = 1.4 - 0.4\,s$ was reported in the literature, this calculation holds only for tetrahedral sites and thus cannot be applied to the present system with five-coordinate iron atoms.[25] However, a shift to larger δ values is known from site-differentiated [4Fe–4S] clusters with coordination numbers greater than four for one of the iron atoms.[2,26] While this has been qualitatively explained by the decrease in spectroscopic oxidation number that results from the electron density provided by the additional donor atom, no quantitative correlation has yet been found.

Furthermore, a surprisingly small quadrupole splitting was observed for **1** (ΔE_Q = 0.43 mm/s). This value was compared to theoretical quadrupole splittings obtained by DFT calculations using two different functionals, namely BP86[27, 28] and B3LYP.[29,30]. Calculations using the crystal coordinates gave lower values than those using the optimized geometry (Table 2), which agrees quite well with the geometry obtained from X-ray diffraction for both BP86 and B3LYP (Table 1). In all cases, a relatively small value was obtained (BP86: 0.18/0.17 (crystal coordinates) and 0.30 mm/s (optimized coordinates); B3LYP: 0.13/0.15 and 0.22 mm/s, respectively); the method without exact exchange (BP86) was closer to the value found experimentally. Although the calculated values are not very exact, the overall trend is correctly reproduced. Like in similar cases,[5,24] calculated values are smaller than experimental values, which therefore seems to be a general trend for [2Fe–2S] clusters when using this DFT method. Compared to other N-coordinated [2Fe–2S] clusters for which quadrupole splittings have been calculated at the BP86 level of theory,[5,24] both the experimental and the calculated value is smallest in case of **1**.

Figure 5. Mössbauer spectrum of **1** at 80 K.

Magnetic susceptibility measurements were performed at 0.5 T from 295 to 2 K (see supporting information for details). As for other [2Fe–2S] clusters, the magnetic moment μ_{eff} decreases upon cooling, indicating a diamagnetic ground state (S_T = 0) with strongly antiferromagnetically coupled ferric ions. The coupling (J = −167 cm^{-1}; see supporting information for details) is in the same range as the coupling determined for clusters with bidentate dipyrromethane ligands.[22] However, the coupling is much stronger than in a cluster with a dithiolate ligand that imposes additional secondary bonding interaction via a chelating thioether group (J = −126 cm^{-1}).[16] Since the relevant distances and angles within the cluster core of the two complexes are very similar (d(Fe· · · Fe) = 2.79 Å as compared to 2.80 Å, α(Fe–μ-S–Fe) = 77.66° as compared to 78.06/78.45°), the differences in magnetic coupling cannot be explained by the geometry of the [2Fe–2S] cluster core alone. Overall, the magnetic properties of the cluster core of **1** seem to be only slightly perturbed compared to those of related systems with bidentate N-donor capping ligands. The coupling constant has also been calculated on both experimental and optimized geometries using the BP86 and the B3LYP functional; the B3LYP calculations gave better results which fit pretty well to the experimental value (BP86: X-ray coordinates: J = −341 cm^{-1} / optimized coordinates: –332 cm^{-1}; B3LYP: −208 cm^{-1} / −154 cm−1; see supporting information for details).

In order to quantify the relative spin distribution over the coordinating atoms, spin densities on relevant atoms were calculated in the ferromagnetically and the antiferromagnetically coupled state for both crystal and optimized coordinates. In addition, these calculations were performed also for the reduced (mixed-valent) state with optimized geometry. Relevant values are listed in Table 3.

In all cases, the spin density is mainly localized on the iron atoms and only little spin density is almost equally distributed over the coordinating N atoms, signifying comparable bond strength (Figure 6).

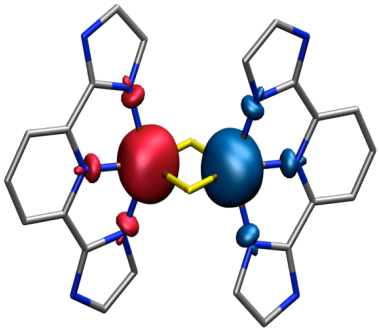

Figure 6. Spin density distribution on **1** (0.01 a.u. contour value; the colours represent alpha and beta spins; results for the AF state, optimized coordinates).

The energy difference between the antiferromagnetic (AF) and ferromagnetic (F) spin states is large for the oxidized state, favoring the AF state which is also the one experimentally found. In the reduced state, however, the energy difference becomes smaller. Unfortunately, all attempts to experimentally isolate a reduced mixed-valent species $[\mathbf{1}]^-$ have failed.

Conclusions

Complex **1** reported here is the first synthetic example of a [2Fe–2S] cluster with genuinely five-coordinate iron atoms. This leads to a slight increase in the Fe· · · Fe distance and Fe–S–Fe angles compared to conventional ferredoxin models. The Mössbauer parameters are also perturbed: the isomer shift is more positive than that of related four-coordinate [2Fe–2S] clusters and the quadrupole splitting is unusually small. Spin density is concentrated on the ferric ions, but equal distribution of delocalized spin densities over all coordinating N atoms obtained from DFT calculations supports a true five-coordinate nature of the iron atoms. This is furthermore confirmed by the line broadening of the pyridine signals in the ^{1}H NMR spectrum. The reduction potential of complex **1** is remarkably positive. An attractive option for future work might be the study of a proton-coupled reduction of **1**, because of the presence of non-coordinating and protonable N atoms in the ligand backbone; this situation bears some resemblance to the histidine-ligated site of Rieske type [2Fe–2S] clusters. Unfortunately, however, the limited stability of **1** in solution has hindered further investigations so far.

While such systems have not yet been discovered in nature, complex **1** provides valuable benchmark data for [2Fe–2S] clusters with five-coordinate metal ions in their oxidized diferric state.

ACKNOWLEDGMENT We thank Jörg Teichgräber for collecting the CV data and Benjamin Schneider for additional Mössbauer measurements. Financial support by the Fonds der Chemischen Industrie (Kekulé fellowship for M.G.G.F.), the Deutsche Forschungsgemeinschaft and the Swedish research council (International Research Training Group GRK 1422 "Metal Sites in Biomolecules: Structures, Regulation and Mechanisms"; see www.biometals.eu) is gratefully acknowledged. The investigation has also been supported by computer resources of Lunarc at Lund University.

Supporting Information Available: Experimental procedures; crystallographic data; details of SQUID measurements (Figure S1); details of DFT calculations (Tables S1–S3); . This material is available free of charge via the internet at http://www.pubs.acs.org.

REFERENCES

1. Beinert, H.; Holm, R. H.; Münck, E., *Science* **1997,** *277*, 653-659.
2. Rao, P. V.; Holm, R. H., *Chem. Rev.* **2004,** *104*, 527-559.
3. Meyer, J., *J. Biol. Inorg. Chem.* **2008,** *13*, 157-170.
4. Ballmann, J.; Dechert, S.; Demeshko, S.; Meyer, F., *Eur. J. Inorg. Chem.* **2009**, 3219-3225.
5. Ballmann, J.; Albers, A.; Demeshko, S.; Dechert, S.; Bill, E.; Bothe, E.; Ryde, U.; Meyer, F., *Angew. Chem.* **2008,** *120*, 9680-9684.
6. Berkovitch, F.; Nicolet, Y.; Wan, J. T.; Jarrett, J. T.; Drennan, C. L., *Science* **2004,** *303*, 76-79.
7. Di Costanzo, L.; Flores Jr., L. V.; Christianson, D. W., *Proteins* **2006,** *65*, 637-642.
8. Lauble, H.; Kennedy, M. C.; Beinert, H.; Stout, C. D., *J. Mol. Biol.* **1994,** *237*, 437-451.
9. Layer, G.; Moser, J.; Heinz, D. W.; Jahn, D.; Schubert, W.-D., *EMBO J.* **2003,** *22*, 6214-6224.
10. Dai, S.; Friemann, R.; Glauser, D. A.; Bourquin, F.; Manieri, W.; Schürmann, P.; Eklund, H., *Nature* **2007,** *448*, 92-98.
11. Hänzelmann, P.; Schindelin, H., *Proc. Natl. Acad. Sci. U. S. A.* **2004,** *101*, 12870-12875.
12. Lepore, B. W.; Ruzicka, F. J.; Frey, P. A.; Ringe, D., *Proc. Natl. Acad. Sci. U. S. A.* **2005,** *102*, 13819-13824.
13. Zhou, C.; Holm, R. H., *Inorg. Chem.* **1997,** *36*, 4066-4077.
14. van Strijdonck, G. P. F.; ten Have, P. T. J. H.; Feiters, M. C.; van der Linden, J. G. M.; Steggerda, J. J.; Nolte, R. J. M., *Chem. Ber.* **1997,** *130*, 1151-1157.
15. Ueyama, N.; Yamada, Y.; Okamura, T.; Kimura, S.; Nakamura, A., *Inorg. Chem.* **1996,** *35*, 6473-6484.
16. Ballmann, J.; Dechert, S.; Bill, E.; Ryde, U.; Meyer, F., *Inorg. Chem.* **2008,** *47*, 1586-1596.
17. Fuchs, M. G. G.; Meyer, F.; Ryde, U., *J. Biol. Inorg. Chem.* **2010**, *15*, 203-212.
18. Stupka, G.; Gremaud, L.; Bernardinelli, G.; Williams, A. F., *Dalton Trans.* **2004**, 407-412.
19. Carina, R. F.; Verzegnassi, L.; Bernardinelli, G.; Williams, A. F., *Chem. Commun.* **1998**, 2681-2682.
20. Do, Y.; Simhon, E. D.; Holm, R. H., *Inorg. Chem.* **1983,** *22*, 3809-3812.
21. Addison, A. W.; Rao, T. N.; Reedijk, J.; van Rijn, J.; Verschoor, G. C., *J. Chem. Soc. Dalton Trans.* **1984**, 1349-1356.
22. Ballmann, J.; Sun, X.; Dechert, S.; Bill, E.; Meyer, F., *J. Inorg. Biochem.* **2007,** *101*, 305-312.
23. Aranzaes, J. R.; Daniel, M.-C.; Astruc, D., *Can. J. Chem.* **2006,** *84*, 288-299.
24. Fuchs, M. G. G.; Dechert, S.; Demeshko, S.; Ryde, U.; Meyer, F., manuscript in preparation.
25. Hoggins, J. T.; Steinfink, H., *Inorg. Chem.* **1976,** *15*, 1682-1685.
26. Ciurli, S.; Carrié, M.; Weigel, J. A.; Carney, M. J.; Stack, T. D. P.; Papaefthymiou, G. C.; Holm, R. H., *J. Am. Chem. Soc.* **1990,** *112*, 2654-2664.
27. Perdew, J. P., *Phys. Rev. B* **1986,** *33*, 8822-8824.
28. Becke, A. D., *Phys. Rev. A* **1988,** *38*, 3098-3100.
29. Becke, A. D., *J. Chem. Phys.* **1993,** *98*, 5648-5652.

30. Stephens, P. J.; Devlin, F. J.; Frisch, M. J.; Chabalowski, C. F., *J. Phys. Chem.* **1994,** *98*, 11623-11627.

Table 1. Selected interatomic distances and angles of **1**.

	d(Fe· · · Fe)/Å	d(Fe–μ-S)/Å	d(Fe–$N_{imidazole}$)/Å	d(Fe–$N_{pyridine}$)/Å	α(Fe–μ-S–Fe)/°	α($N_{imidazole}$–Fe–$N_{imidazole}$)/°	α(Fe· · · Fe–$N_{pyridine}$)/°	τ_5[a]
experimental	2.7911(3)	2.2136(4) 2.2377(4)	2.1139(16) 2.1177(13)	2.1799(12)	77.660(14)	141.300(56)	162.81(3)	0.085
calculated (BP86)	2.78	2.24 2.22	2.16	2.22	77.2	140.3	161.3	0.12
calculated (B3LYP)	2.92	2.28 2.27	2.17	2.24	79.9	139.6	161.6	0.15

a) Calculated according to $\tau_5 = (\beta-\alpha)/60°$ with α and β being the two largest bond angles.[21]

Table 2. Selected electrochemical and spectroscopic data of complex **1**.

λ_{max}/nm	ε/(l/(mol· cm))	$E_{1/2}$[a]/V	δ/(mm/s)	ΔE_Q/(mm/s)	ΔE_Q(calc.)[b]/(mm/s)	ΔE_Q(calc.)[c]/(mm/s)
310, 370, 489	34000, 10000 (sh), 3000	−0.52[d]	0.44	0.43	0.18/0.17 (BP86) 0.13/0.15 (B3LYP)	0.30 (BP86) 0.22 (B3LYP)

a) Reduction potentials were measured vs. the $Cp^*_2Fe/Cp^*_2Fe^+$ couple and referenced vs. NHE.[23] b) Calculated quadrupole splittings were obtained from the eigenvalues of the electric field gradient at the positions of the iron atoms using crystal coordinates. c) Calculated quadrupole splittings were obtained from the eigenvalues of the electric field gradient at the positions of the iron atoms for an optimized geometry. d) ΔE = 70 mV ($Cp^*_2Fe/Cp^*_2Fe^+$: ΔE = 87 mV).

Table 3. Calculated spin densities on relevant atoms of **1**.[a]

				ρ/a.u.			
	functional	coupling	$E_{relative}$[b]/(kJ/mol)	Fe	S	$N_{pyridine}$	$N_{imidazole}$
crystal coordinates							
1	BP86	F	+106	3.91	0.76	0.05	0.07
		AF	0	3.62	0.04	0.05	0.05
	B3LYP	F	+63	4.02	0.72	0.04	0.07
		AF	0	3.94	0.03	0.05	0.06
optimized coordinates							
1	BP86	F	+81	3.97	0.75	0.04	0.06
		AF	0	3.66	0.03	0.05	0.05
	B3LYP	F	+40	4.06	0.71	0.04	0.06
		AF	0	4.00	0.03	0.04	0.06
$\mathbf{1}^{reduced}$	BP86	F	+25	3.78	0.53	0.03	0.04
		AF	0	3.72/−3.50	0.18/0.22	0.03	−0.03/0.04
	B3LYP	F	+5	3.89	0.48	0.02	0.03
		AF	0	−3.77/3.97	0.39/0.30	0.02	0.02/0.04

a) Spins are calculated at two levels of theory (BP86 and B3LYP) for the ferromagnetic (F) or antiferromagnetic (AF) states. The oxidized state was considered for crystal and optimized coordinates, the reduced state only for optimized coordinates. When only one value is given, the value on the other respective atom was equal or the negative equivalent; the $N_{imidazole}$ atoms are considered as two pairs of similar atoms. b) The energy difference between the F and AF states; see supporting information for details.

Graphical Contents Entry:

A unique [2Fe–2S] cluster (**1**) with genuinely five-coordinate iron atoms has been synthesized and investigated both structurally and spectroscopically. The crystal structure of **1** as well as ^{1}H NMR data reveal that 2,6-bis(imidazol-2-yl)pyridine binds to the [2Fe–2S] core as a tridentate capping ligand. DFT calculations showing spin density on all coordinating atoms support this finding.